

# Benchmark calculations for electron velocity distribution function obtained with Monte Carlo Flux simulations

L. Vialetto<sup>1</sup>, S. Longo<sup>2</sup>, P. Diomedede<sup>1,\*</sup>

<sup>1</sup>*Center for Computational Energy Research, DIFFER – Dutch Institute for Fundamental Energy Research, De Zaale 20, 5612 AJ Eindhoven, the Netherlands*

<sup>2</sup>*Dipartimento di Chimica, Università degli Studi di Bari, via Orabona 4, 70126 Bari, Italy*

\*corresponding author, e-mail: p.diomedede@differ.nl

## Abstract

Modern, multi-modular plasma modeling requires accurate and versatile methods for the determination of the electron velocity distribution function from which rate coefficients of electron impact processes as well as electron transport quantities are determined. In this paper we propose as a solution a modified version of a strongly overlooked method developed in the early 90's, namely, Monte Carlo Flux (MCF). The improvement lies in a criterion for the otherwise somewhat empirical selection of the time-step used in the method. We show that an MCF based code highlights and overcomes the limitations of two-terms codes such as BOLSIG+ and it is much faster than a conventional Monte Carlo. Moreover, MCF is in excellent agreement with the multi-term method for a wide range of reduced electric fields, being at the same time much simpler to implement and to extend to more general cases than the latter. Explicit illustrations of the Markov matrices representing short-time kinetics are presented to gain insight into the method. The two-dimensional velocity distribution and its expansion into Legendre polynomials are discussed for electrons in argon.

**Keywords:** Electron Boltzmann equation, Monte Carlo Flux, electron energy distribution function, Legendre polynomials coefficients.

## 1. Introduction

In the past decades, great progress has been made in the field of technological applications of low-temperature plasma physics and chemistry. An example is information technology, with the miniaturization of integrated circuits and functionalization of materials [1, 2]. Nowadays, plasma technologies are exploited in bio-medical [3] and environmental [4] applications and became indispensable in many other fields. A detailed overview on the status and challenges of the field can be found in recent reviews [5, 6].

An important feature of low-temperature plasmas is that they can be often far from thermodynamic equilibrium, that is the average energy of the electron population is much larger than the one for heavy particles [7]. The dynamics of non-equilibrium plasmas is dominated by electrons that are fundamental to sustain the discharge through collisional processes. For example, ionization by free electrons is a key mechanism for sustaining the discharge. Moreover, excitation and de-excitation processes give an important contribution to the production or loss of chemically active species. To this end, a detailed understanding and knowledge of the complex plasma physics and chemistry mechanisms is desirable for the control and optimization of plasma-based technologies. This complexity requires numerical models for the description of the main reaction channels, as discussed in details in [7, 8]. In plasma regimes dominated by short range interactions, knowledge of the electron distribution function is essential to calculate chemical rate coefficients, as well as electron transport parameters. A comprehensive review of established techniques and recent progresses in electron distributions descriptions can be found in [9].

Distribution functions for electrons are generally obtained by numerically solving the corresponding Boltzmann equation. In this context, two different methods are mostly used to investigate electron dynamics: deterministic solution of the Boltzmann equation and Monte Carlo (MC) method. On the one hand, the former is based on different implicit and explicit approximations for the solution of the Boltzmann equation, for example, the two-term approximation, that is typically valid under the hypothesis of small anisotropy of the electron distribution function in velocity space. A widely employed code, based on the two-term approach, is BOLSIG+ [10, 11], that is also used in the PLASIMO [12, 13] and ZDPlasKin [14] codes. Other research groups employing codes based on the two-term approximation are the Lisbon group [15-18], the Bari group [19] and Dyatko and co-authors [20], to study electron kinetics in atomic and

molecular plasmas. In this respect, it is worth to mention the LoKI-B code that has recently been released as open source and can be used to solve a space and time independent form of the two-term Boltzmann equation [21, 22]. Other examples of two-term solvers are EEDF [23] and BOLOS [24]. Extension to multi-term solution techniques is widely established for the calculation of accurate distribution functions and transport parameters. In this respect, great advances have been made by Robson and co-authors [25-27], Pitchford and co-authors [28], Dujko and co-authors [29] and the Greifswald group [30]. Recently, the multi-term solver MultiBolt has been developed and distributed as an open source code [31].

On the other hand, MC methods are propagation methods based on statistical laws of probabilities. In MC simulations, individual particles are traced and collisions are simulated as stochastic processes using random numbers. A description of MC methods for charged particles and their derivation from the transport equation can be found in [32-34]. Moreover, applications of MC to simulations of electrons can be found in [35-37]. An example of open source MC code for electron transport is METHES [38, 39]. Vast literature can be found on the comparison of different methods based on the deterministic analysis and MC in terms of accuracy and calculation of swarm transport parameters (e.g. [40-42]). The advantage of the MC method is that it can be easily applied to different conditions, even when the deterministic analysis becomes cumbersome, but it may require large computational times.

Variance reduction techniques are usually employed to reduce the computational load [43]. An example is Monte Carlo Flux (MCF). This method was originally proposed by Schaefer and Hui for solving the electron transport problem [44] and applied in few other works mainly by Longo and Capitelli [45]. An extension of the method called generalized MCF was also proposed by Wu and co-authors [46]. Despite the little attention this method received with respect to other techniques, MCF offers the possibility of computing electron velocity distribution functions ranging over several orders of magnitude, a feature that can be matched in MC only employing variance reduction techniques. At the same time, as it will be seen later, MCF allows to treat optimally the much different timescales of collision and relaxation using MC only for the former, where it performs best. In this respect, the base idea of MCF is the reduction of the number of simulated collisions, as it will be explained in Section 2. This makes this method computationally efficient.

In this work, an implementation of MCF optimized for fast and accurate calculations of electron dynamics is presented. The emphasis is on the influence of numerical parameters on the accuracy of results. This is an important step for a future possible integration of an MCF solver in a more sophisticated chemistry model. Furthermore, results are validated against an analytical solution and against solutions based on two-term and ten-term expansion in Legendre polynomials. The paper is structured in the following way: in section 2, theoretical bases of the MCF method are illustrated. In section 3, details about code implementation are presented. In section 4.1, optimization of numerical parameters and validation against an analytical solution are discussed. In particular, an improved criterion for the calculation of the MC time step is presented and it is shown that, in this way, the method can be exploited for simulations in several conditions. In section 4.2, a benchmark of the MCF code against the two-term solver BOLSIG+ and the multi-term solver MultiBolt is presented, in particular as far as the calculation of Legendre polynomial coefficients is concerned. Calculations are performed for the case of argon chemistry for a wide range of values for the reduced electric field. An example of steady-state solution of the electron velocity distribution function in 2D velocity space is shown at the end of section 4, together with the time evolution of the EEDF, in order to illustrate additional capabilities of MCF simulations.

## 2. Numerical methods to solve the electron Boltzmann equation

Non-equilibrium plasmas modelling requires the knowledge of the distribution function for free electrons that can be obtained as a numerical solution of the corresponding Boltzmann equation:

$$\left[ \frac{\partial}{\partial t} + \mathbf{v} \cdot \nabla_{\mathbf{r}} + \mathbf{a} \cdot \nabla_{\mathbf{v}} \right] f(\mathbf{r}, \mathbf{v}, t) = \left( \frac{\partial f}{\partial t} \right)_{coll}. \quad (1)$$

Eq. (1) describes the time evolution of the electron distribution function  $f(\mathbf{r}, \mathbf{v}, t)$  in phase space under the effect of space and velocity gradients, the acceleration  $\mathbf{a}$ , due to external forces and collisions, described by the term on the right hand side. From the distribution function, it is possible to calculate macroscopic quantities useful to characterize the discharge properties [47].

In what follows, a particular form of Eq. (1), the so called linear Boltzmann equation [48], is solved numerically. In this equation, the gas is diluted enough, so that only binary interactions between electrons and heavy particles are taken into account. Collisions are also assumed to be instantaneous, therefore the effect of any external force is negligible during a collision event. A

homogenous and constant electric field is considered, acting along the  $\hat{z}$ -direction on the electrons ensemble. Moreover, an infinite gas where all quantities in Eq. (1) are independent on space variables (homogenous problem) is assumed. In those conditions, the electron distribution function is dependent only on time and 2D velocity-space coordinates (i.e. axial and radial velocity component), or alternatively on energy and direction of the velocity vector with respect to the electric field. This is the so called Electron Velocity Distribution Function (EVDF). Under conditions of axial symmetry in velocity space around the direction of the electric field, the EVDF  $f(\varepsilon, \cos \theta, t)$  is usually expanded in series of Legendre polynomials  $P_l(\cos \theta)$ :

$$f(\varepsilon, \cos \theta, t) = \sum_{l=0}^{\infty} f_l(\varepsilon, t) P_l(\cos \theta), \quad (2)$$

where  $\theta$  is the angle between the direction of the velocity vector and of the electric field,  $\varepsilon$  is the electron energy and  $f_l(\varepsilon)$  is the  $l$ -th order Legendre polynomial coefficient in the expansion. This procedure is limited to spatially-homogenous conditions driven by an electric field. More generally, an expansion in spherical harmonics in velocity space is used in case of spatial inhomogeneity or in absence of axial symmetry [42].

A set of ordinary differential equations is then solved, one for each term in the Legendre expansion. Usually only two terms ( $f_0(\varepsilon)$  and  $f_1(\varepsilon)$ ) are taken into account, where  $f_0(\varepsilon)$  is usually referred as the isotropic component or Electron Energy Distribution Function (EEDF) and it is used in the calculation of chemical rate coefficients and flux transport parameters [47]. This is referred in literature as two-term approximation. This approximation is satisfied for relatively small energy variations in elementary processes, for example in cases of large diffusion by elastic collisions. The truncation of the expansion in two terms is possible because of the small electron to heavy particles mass ratio  $m/M$  [49]. In general, for values of electric fields that enhance the role of inelastic collisions, higher orders in the Legendre polynomial expansion must be taken into account [50]. Another limitation of a two-term approach concerns the distribution of scattered electrons, where inelastic collisions are treated as isotropic [51]. Those limitations are overcome in multi-term solvers, at the cost of numerical complexity [28]. Multi-term solvers are also widely used to obtain accurate calculations of swarm transport parameters, in conditions where the two-term approximation breaks down [29].

An alternative under such conditions is the MC method [32, 34] in which the electrons motion is simulated in phase space under the effect of external forces and binary interactions. Usually, the null-collision method is employed to calculate the time between two successive collisions as a

Poisson stochastic process [52]. Accuracy and versatility are other advantages of MC, that is also useful when space-dependent quantities are sought and the local field approximation cannot be applied due to non-local effects of electron kinetics [47]. Despite its advantages, a drawback of MC is the high computational cost needed to obtain a solution with a reduced level of statistical error. In fact, stochastic fluctuations scale slowly with the number of particles  $n$  as  $n^{-1/2}$ . Additionally, being equivalent to a direct, time dependent solution of the Boltzmann equation, it suffers the very different time scales of collision and relaxation, which are in the same ratio as  $m/M$ . In fact, while the typical collision time is mostly determined by the momentum relaxation frequency, the relaxation time of the distribution function depends on the energy relaxation frequency, that is typically much lower [53]. This mass mismatch is usually not a problem due to the different way electron kinetics is treated in a Fokker-Planck formulation of the Boltzmann equation and in a Monte Carlo model. However, it can be a real problem under conditions where the  $m/M$  ratio is the bottleneck of the time evolution: for example, in a post-discharge situation, the energy drift downwards in the region of elastic collisions is due to a term proportional to  $m/M$  and this applies also to any single collision in MC.

Variance reduction techniques [43] are employed to reduce statistical noise due to stochastic fluctuations in the distribution function. These techniques are based on using variable mathematical weights for particles in various ways, while increasing the number of particles in regions of phase space, or increasing the number of useful calculations performed during the particle simulation. These techniques, however, cannot address the fundamental problem of the very large ratio, amounting to several orders of magnitude, between the relaxation time of the distribution and the inter-collision time. In fact, MC methods are intrinsically time-dependent and describe the electron history from collision to collision and because of this large ratio they are highly computationally expensive even when the problem of phase space coverage is optimally dealt with. A very efficient alternative to traditional variance reduction techniques is the Monte Carlo Flux (MCF) [44]. The MCF procedure consists of three steps. The first step is the subdivision of the velocity domain in cells. For instance, for the 2D axisymmetric case, each cell is uniquely identified by a couple of indexes  $(i, j)$  corresponding to different energy ( $\varepsilon$ ) and  $\cos \theta$  bins, determined by:

$$(i - 1)\Delta\varepsilon \leq \varepsilon < i\Delta\varepsilon, \quad i = 1, \dots, n_\varepsilon \quad (3)$$

$$(j - 1)\Delta(\cos \theta) \leq \cos \theta < j\Delta(\cos \theta), \quad j = 1, \dots, n_{\cos \theta},$$

where  $n_\varepsilon$  and  $n_{\cos \theta}$  are the number of bins in the energy and angular domain, with size  $\Delta\varepsilon$  and  $\Delta(\cos \theta)$ , respectively. The simulation is initiated by placing a distribution of electrons at time  $t = 0$  in each cell of the velocity space, such that, for example,  $N_{(1,1)}(t = 0)$  represents the number of electrons initially inserted in the  $(i = 1, j = 1)$ -cell. In the second step, the initial electron distribution is evolved in time through an MC simulation. In particular, during a time interval  $\Delta t$ , electrons move between velocity space cells due to the presence of the electric field and undergo stochastic collision processes. The information about electron transport between cells can be captured by defining the conditional transition probabilities between velocity space cells:

$$p_{I \rightarrow J}(\Delta t) = N_{I \rightarrow J}(\Delta t) / N_I(t = 0). \quad (4)$$

Where  $I$  and  $J$  are indexes identifying two different bidimensional cells associated, for example, with the  $(i, j)$ -th and  $(k, l)$ -th cell respectively. In this way,  $p_{I \rightarrow J}(\Delta t)$  is the transition probability for electrons moving from cell  $I$  to cell  $J$  in the time interval  $\Delta t$  and it is calculated as the ratio between the number  $N_{I \rightarrow J}$  of electrons moving from cell  $I$  to cell  $J$  and the total number of electrons inserted in cell  $I$  at time  $t = 0$ . Transition probabilities between velocity space cells can be conveniently represented in terms of a matrix, also known as Markov matrix, that can be used for computations of time evolutions and steady-state solutions. In the third step, a Master Equation (ME) which describes the deterministic time evolution of the EVDF, is generated by subsequent applications of the Markov matrix to the initial electron distribution. In fact, a ME can be written for each velocity space cell as:

$$\Delta N_I(t) = \sum_J p_{J \rightarrow I}(\Delta t) N_J(t) - N_I(t) \sum_J p_{I \rightarrow J}(\Delta t). \quad (5)$$

The time evolution of the electron distribution with time step  $\Delta t$  is obtained by an iterative application of Eq. (5). As an alternative, the steady-state solution can also be calculated as the eigenvector associated to the unitary eigenvalue of the Markov matrix [44].

An important consequence of Eq. (5) is that the evolution of the system after  $\Delta t$  is determined only by the state of the system at a time  $t$  and it is not affected by the previous history. This is known as Markov property and allows one to rewrite the linear Boltzmann equation as a simple Markov chain consisting of the system of linear equations in Eq. (5) [5354]. This property is typically satisfied if

$$\tau_{coll} \ll \Delta t \ll \tau_{SS}, \quad (6)$$

that is  $\Delta t$  should be much longer than the collision time  $\tau_{coll}$ , but typically orders of magnitude shorter than the time  $\tau_{SS}$  for the distribution function to reach steady-state [47]. In fact, collisions are essential for the randomization of the particle velocities and trajectories. Through this randomization, electron history is erased and the evolution of the system depends only on the current state, not on past states. To summarize, the MCF method has three main advantages. First of all, electrons trajectories are followed only for a limited time interval  $\Delta t$ , typically orders of magnitude shorter than the relaxation time of the distribution. In this way, while the capability of reducing computational cost can be matched by more complex variance reduction techniques, MCF differs from any other MC solution in the possibility of avoiding the calculation of a sometimes huge number of collisions. This introduces a great simplification in the electron transport problem in which the time evolution of the electron distribution function is simulated as a discrete Markov process described by the transition probabilities. In addition, transition probabilities can be determined even in high energy regions. This leads to a significant reduction of stochastic fluctuations in the calculation of the electron velocity distribution function, that cannot be obtained by conventional MC approaches without simulating a large sample of electrons. This aspect is highly beneficial, for example, in the calculation of chemical rate coefficients of inelastic processes with a threshold in the energy range of the tail of the distribution. The third advantage lies in the fact that MCF does not make any assumption on the type of transport and, in particular, it is not limited to small energy variations that are typically assumed in a two-term approach.

Of course, MCF also presents limitations, and these must be taken into account when choosing an appropriate method between MCF and traditional alternatives for a specific application. The main limitation of MCF is the necessity of constant reduced electric field  $E/N$  during time evolution, because any recalculation of transition probabilities requires a new MC calculation. Of course, this limitation can be solved in some cases, such as for example in periodic variations of  $E/N$  or a single switch-on or switch-off of the field, but, in cases where variations are fast (that is  $E/N$  is changing significantly during the EVDF relaxation time), the straightforward MC method could be a preferred method. Additionally, the code development and management for MCF is undoubtedly more complex than those of alternatives like plain MC and two-term Boltzmann solvers.



Therefore, the gain in efficiency and the additional information must be relevant in the considered application, to compensate for this cost.

In perspective, MCF can be integrated in codes describing chemical kinetics, such as global models. In this framework, recalculations of transition probabilities are necessary if the gas composition is changing in the time scales under examination.

### 3. Code implementation

An MCF implementation was carried out together with a criterion for the calculation of the time step which was not present in the original paper by Schaefer and Hui [44]. The code is written in Fortran 95/2003 with the use of modern features like derived data types and modules. The core of the code consists of three parts: a discretization module to partition the velocity space by means of a mesh; a Monte Carlo module to calculate transition probabilities; a Markov chain module to solve the discretized transport equation (Eq. (5)).

#### *Discretization module*

The choice of a mesh in velocity space is fundamental in MCF for defining the discretized transport equation (Eq. (5)). By means of the mesh, the electron distribution function is rewritten as a discrete set of states, each representing the number of electrons in each cell. Moreover, transition probabilities between velocity space cells can be calculated. For simplicity, here equally spaced cells are considered, each having size  $\Delta v$  in the  $v$ -direction. However, the use of adaptive mesh refinements and/or different discretization schemes may have advantages for studies of electron transport at high E/N and for a possible future extension of the present method to the configuration space. In practice, a one dimensional grid in energy ( $\varepsilon$ ) is sufficient if the only interest is the computation of the EEDF, neglecting angular dependencies of the distribution function. In the more general case of axial symmetry around the direction of the electric field, a 2D grid in ( $\varepsilon, \cos \theta$ ) can be considered. A given number of electrons at time  $t = 0$  is inserted in each cell. This is an important feature of MCF: transition probabilities can be calculated even between high energy cells by inserting electrons in the whole velocity space. Typically, in the simulations presented here, 1000 velocity space cells are used, with a uniform distribution of  $10^4$  or  $10^5$  electrons per cell. This leads to the calculation of  $1000 \times 1000$  conditional transition probabilities between cells, that are computed with the Monte Carlo module described in the next paragraph.

### *Monte Carlo module*

The aim of this module is the calculation of conditional transition probabilities of electrons moving in velocity space cells (Eq. (4)). Each electron, initially located in a specific velocity space cell, moves under the effect of the electric field and undergoes collisions with the background gas. This motion is described by MC simulations. However, as opposed to conventional MC approaches, the stochastic part is limited to a time step  $\Delta t$  [44]. After  $\Delta t$ , the time evolution is calculated deterministically by a Markov chain. As previously stated, this time interval is usually orders of magnitude lower than the MC steady-state time (Eq. (6)).

In the MC module, the modified time step technique is implemented as propagation method [34, 55]. Binary collisions between electrons and neutrals are simulated as Poisson stochastic processes, where the time between two successive collisions is computed using the null collision method introduced by Skullerud [52]. A Fortran translation of the 64-bit version of the Mersenne Twister pseudorandom number generator is used [56-58]. Explicit effects of non-conservative collision processes are taken into account. In particular, in case of ionization collisions, formation of secondary electrons is included until reaching a given maximum number of particles. In that case, a random electron is removed from a dynamic list of simulated particles. This method has been proposed and tested in previous works, such as [62].

Transition probabilities are stored in a matrix, where row indexes represent initial states of electrons inserted in velocity space at time  $t = 0$  and column indexes represent final states calculated after a time  $\Delta t$ . If the number of electrons is conserved, the sum of elements in each row of the matrix is equal to 1. In this specific case, a Markov matrix is obtained which has always an eigenvalue equal to 1, whose eigenvector represents the stationary solution of the problem. The Markov matrix contains transition probabilities calculated considering the contribution of each electron initially placed in velocity space. For this reason, it is clear that this module is the most computationally expensive part of the MCF code. However, the real power of the method is the possibility of storing transition probabilities and using a deterministic approach to calculate time evolution and, eventually, a steady-state solution. This is obtained by means of the Markov chain module.

### *Markov chain module*

The use of a grid in velocity space allows us to rewrite the transport problem of Eq. (1) as a system of linear equations used to calculate the discretized velocity distribution function. Calculations of steady-state distributions are performed in this module with an eigenvalue method using the DGEEV subroutine of the LAPACK 3.8.0 library [59]. The typical computational time of this routine spans from milliseconds for a  $10^2 \times 10^2$  matrix to a few seconds for a  $10^3 \times 10^3$  matrix, with the Fortran compiler Intel(R) Xeon(R) CPU E5-2637 v3 @ 2.50 GHz. Alternatively, the time evolution could be obtained by iteratively solving the system of equations in Eq. (5) with the use of a sparse matrix solver (e.g. [60]).

A schematic of the MCF implementation is shown in Fig. 1. The simulation is initiated by defining physical parameters, that is cross sections, gas composition and reduced electric field  $E/N$ . In addition, numerical parameters are defined, that is energy and angular bin size ( $\Delta\varepsilon$  and  $\Delta(\cos\theta)$  respectively), initial number of electrons in each cell ( $n_c$ ) and maximum energy range ( $\varepsilon_{max}$ ). The discretization module takes care of the definition of the mesh and coordinates of each cell that are important for the subsequent computation of the Markov matrix. The modified time step technique is used in the MC for the simulation of the motion of each electron for a time  $\Delta t$ . Criteria for the calculation of  $\Delta t$  are illustrated in detail in the next section. This calculation is done adaptively within the current code implementation, depending on simulation conditions. Within the MC module, the Markov matrix is computed and stored. This matrix is then used in the iterative application of the Markov chain to obtain steady-state or time-dependent distribution functions.

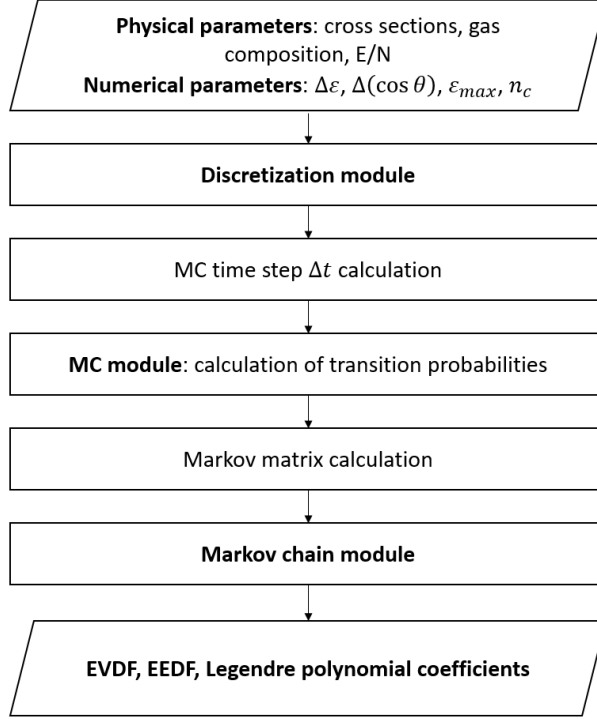


**Fig. 1.** MCF schematic including input/output and the different modules involved in the calculations. See text for a detailed description of modules and functionalities.

## 4. Results

### 4.1 Optimization of numerical parameters

A fundamental advantage of MCF is the possibility to obtain fast and accurate calculations of transition probabilities that can be used iteratively in the Markov chain. These last depend on the choice of the MC time step ( $\Delta t$ ), therefore it is important to study the effect of  $\Delta t$  on the distribution of transition probabilities in velocity space and to identify a general criterion for the choice of the optimal value of  $\Delta t$ .

In order to address this problem, simulations were initially performed for the case of an ideal atomic gas with mass  $A = 4$  amu. Isotropic elastic scattering is assumed with a constant elastic momentum transfer cross section equal to  $2 \times 10^{-20} \text{ m}^2$ . A reduced electric field of 2 Td is applied along the  $\hat{z}$ -direction. With these assumptions, the Druyvesteyn distribution is obtained at steady-state. In terms of numerical parameters, a one dimensional grid in energy with 100 equally spaced

bins of size 0.3 eV is considered. This leads to a  $10^2 \times 10^2$  transition probabilities matrix. A uniform initial distribution of  $10^4$  electrons per bin is assumed, for a total of  $10^6$  electrons in the whole domain. The choice of those numerical parameters is based on the requirement to obtain a relative error for the average properties of the distribution function (i.e. mean energy and rate coefficient) with respect to the analytical solution that does not exceed  $10^{-3}$ .

In Fig. 2, the distribution of transition probabilities in the Markov matrix with different time steps is shown. Starting from a diagonal matrix at time  $t = 0$ , electrons ‘jump’ between energy space cells within the time step  $\Delta t$ . This temporal evolution spreads the initial distribution of transition probabilities to the adjacent cells. In Fig. 2(a), it is shown that for  $\Delta t = 10^{-7}$ s, electrons have time to perform only a few collisions, therefore they move towards adjacent cells only. This preserves an overall diagonal-banded structure. When the time step is increased to  $\Delta t = 10^{-6}$  s, electrons undergo more collisions, causing a diffusion of transition probabilities towards lower energies that are represented by the first few columns of the matrix in Fig. 2(b). The effect of this collisional diffusion is enhanced for longer values of  $\Delta t$ . In fact, at  $\Delta t = 10^{-5}$ s (Fig. 2(c)), all transition probabilities are located in the first few columns of the matrix. This leads to the conclusion that higher values of time steps lead to a poor estimation of transition probabilities between high energy cells. A discussion about the optimal value of  $\Delta t$  and the average number of collisions needed for an accurate estimation of transition probabilities is presented in the next subsection, together with a criterion for the choice of an optimal MC time step.

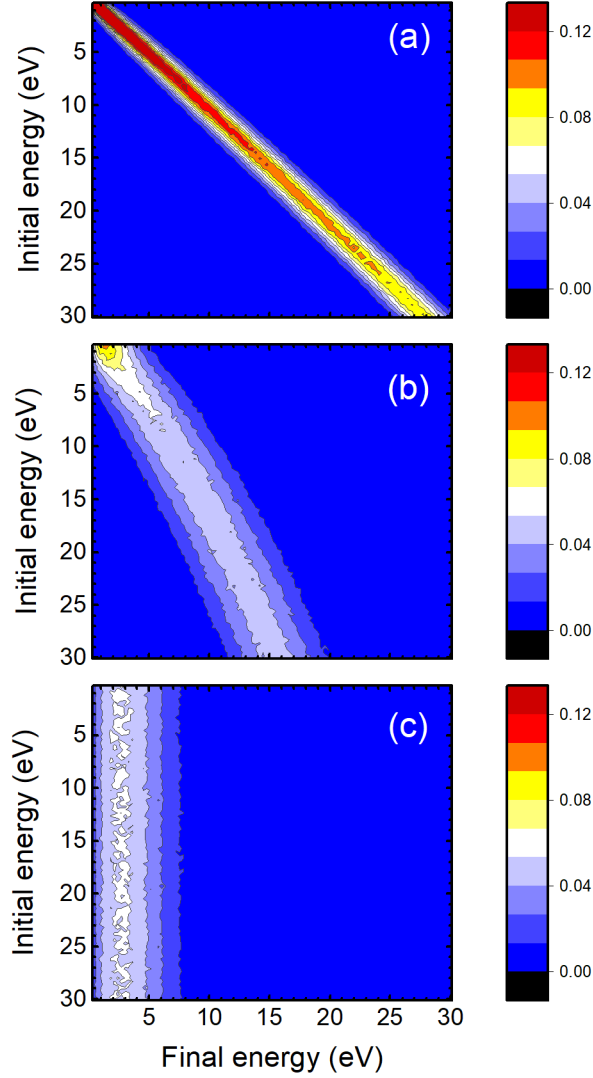


**Fig. 2.** Transition probabilities in the Markov matrix for three different values of time step  $\Delta t$  ((a)  $10^{-7}$  s, (b)  $10^{-6}$  s and (c)  $10^{-5}$  s) for isotropic elastic scattering at 2 Td and a constant cross section of  $2 \times 10^{-20} \text{m}^2$ , an energy bin size of 0.3 eV and 100 energy bins.

In addition, in Fig. 3, it is shown that the choice of  $\Delta t$  has an impact on the calculation of the EEDF. In fact, it can be noted how, in the tail of the distribution, accuracy decreases and stochastic fluctuations increase with time step. In this case, the optimal value of  $\Delta t$  is estimated to be around  $10^{-7} \text{s}$  (with an accuracy for the distribution that spans over 15 orders of magnitude), whereas an increase of the optimal value by one or two orders of magnitude leads to EEDFs that are limited in the tail estimation by the total number of electrons simulated.

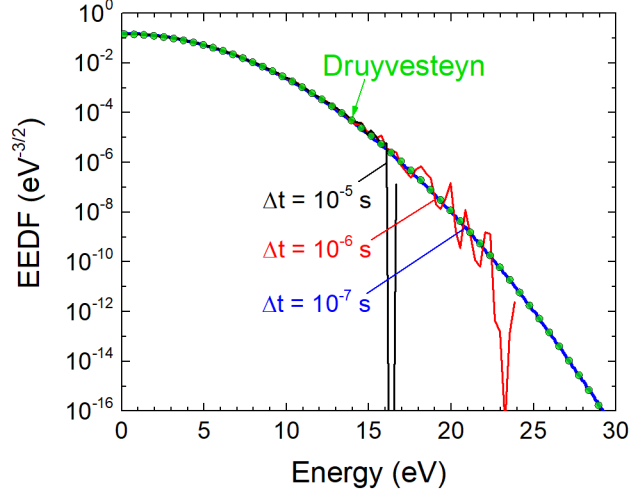


**Fig. 3.** Steady-state EEDFs obtained with MCF for different values of time step. Same conditions as Fig. 2. The analytical Druyvesteyn distribution is also shown (green dots).

In summary, the aim of MCF is to reduce the number of simulated collisions by choosing a value of  $\Delta t$  low enough to obtain accurate transition probabilities even between high energy cells. However, in the next paragraphs, it is shown that  $\Delta t$  cannot be arbitrarily low. In this framework, there is an optimal value for  $\Delta t$  that should be estimated with a robust criterion. This is illustrated in the next part, where the definition of time step is framed in the more general context of a Markov chain.

#### *Criteria for the choice of the time step*

As previously shown, the distribution of transition probabilities reflects the transport of electrons in velocity space. This transport is, in turn, affected by the presence of the external electric field and by collisional processes. However, the two contributions have an opposite effect on the overall electron motion. While collisions tend to randomize the magnitude and direction of velocity vectors, the presence of the electric field tends to create an ordered flow of particles. Such flow can give rise to a “memory effect” and alter the transition probabilities calculated at later times. This violates the Markovian assumption implicit in the MCF method [54]. However, this effect is small provided enough diffusion through collisions takes place within the time step  $\Delta t$ . The problem with MCF is then to find an optimal value of  $\Delta t$ , short enough to allow a reduction of computational cost, but at the same time long enough to ensure that a reasonable number of collisions occur.

In [44], it is suggested that a possible criterion for the optimal  $\Delta t$  is that the velocity component in the electric field direction changes at least by an amount corresponding to the width of the cell in energy space in that direction. In what follows, this condition is called ‘*Criterion 1*’ to differentiate it from another one introduced later. In order to compute  $\Delta t$  according to Criterion 1, electrons are initially placed in the first energy bin and are evolved in time until the following condition is met:

$$|v_z| \geq \sqrt{2\Delta\varepsilon/m}, \quad (7)$$

where  $|v_z|$  is the magnitude of the velocity component along the direction of the electric field and  $m$  is electron mass. The average time interval calculated from the contribution of each electron is used as time step  $\Delta t$  for the Monte Carlo module. It was found that at least  $10^3$  electrons are needed to have a significant statistical sample for the average calculation. This is an empirical criterion that can be applied in most cases. In fact, such a criterion captures the dynamics well, but not in conditions where drift due to the electric field is dominant over diffusion due to collisions. In that case, Criterion 1 may lead to values of  $\Delta t$  lower than the typical collision time, thus preventing any randomization of the velocity vectors. This is a problem for MCF, since the Markovian assumption breaks down. In a drift regime dominated by the presence of electric field, it was found that the energy bin size is limited by the following relation:

$$\Delta\varepsilon \geq e \frac{E/N}{\sqrt{2}\sigma}, \quad (8)$$

where  $E/N$  is the reduced electric field in  $\text{V}\cdot\text{m}^2$ ,  $e$  is the elementary charge and  $\sigma$  is the total collisional cross section (in  $\text{m}^2$ ) for electrons in the first energy bin. Relation (8) is an empirical formula with a straightforward meaning: the energy bin size should be large enough for at least one collisional process to occur within the time it takes an electron (on average) to drift towards adjacent energy cells. When condition (8) is not fulfilled, the Markovian assumption does not hold, since not enough collisions are simulated. In order to avoid the use of a coarse mesh, even at high values of  $E/N$ , a second criterion is introduced and applied only in cases where relation (8) is not valid: this is called *Criterion 2*. In this new criterion, together with relation (7), it is required that each of the  $10^3$  sample electrons inserted in the first energy bin undergoes at least a few collisions within the time step. It was found that a minimum of 50 collisions performed by each electron is a good compromise between accuracy and computational cost.



In order to check Criterion 2 and comparing it with Criterion 1, the ideal gas with isotropic elastic scattering and  $\sigma = 2 \times 10^{-20} \text{m}^2$ ,  $E/N = 50 \text{ Td}$  previously examined, was modeled again. In this case, condition (8) is verified by using an energy bin size larger or equal than 1.8 eV. For  $\Delta\varepsilon = 1.8 \text{ eV}$ , Criterion 1 holds and a value of  $\Delta t = 1.4 \times 10^{-7} \text{s}$  is obtained. Results with those numerical parameters, were in excellent agreement with the theoretical Druyvesteyn distribution (not shown). On the other hand, for  $\Delta\varepsilon = 1.0 \text{ eV}$ , condition (8) is not fulfilled, thus Criterion 2 is more appropriate than Criterion 1 to describe the system under investigation. A value of  $\Delta t = 6.5 \times 10^{-7} \text{s}$  is calculated with Criterion 2, whereas a value of  $\Delta t = 1.1 \times 10^{-7}$  is derived from Criterion 1. As expected, in this case, the EEDF calculated with Criterion 1 deviates from the analytical solution, instead the calculation with Criterion 2 gives a distribution in agreement with the analytical solution in the whole energy range (Fig. 4(a)). Deviations from the analytical solution can be better evaluated by estimating the percent error of MCF results with respect to the Druyvesteyn distribution. This is calculated as  $\Delta f_0(\varepsilon)/f_{0,Druyv.}(\varepsilon) = (f_0(\varepsilon) - f_{0,Druyv.}(\varepsilon))/f_{0,Druyv.}(\varepsilon)$ , where  $f_0$  is the EEDF calculated from MCF and  $f_{0,Druyv.}$  is the analytical Druyvesteyn distribution, and it is shown in Fig. 4(b). A maximum energy of 400 eV was considered, where the distribution function reaches values below  $10^{-7} \text{ eV}^{-3/2}$ . It is evident that Criterion 1 gives rise to a systematic deviation from the analytical distribution. Moreover, even if with a small statistical noise in the tail, Criterion 2 outperforms the first one by keeping the relative error within 3% in the whole energy range.

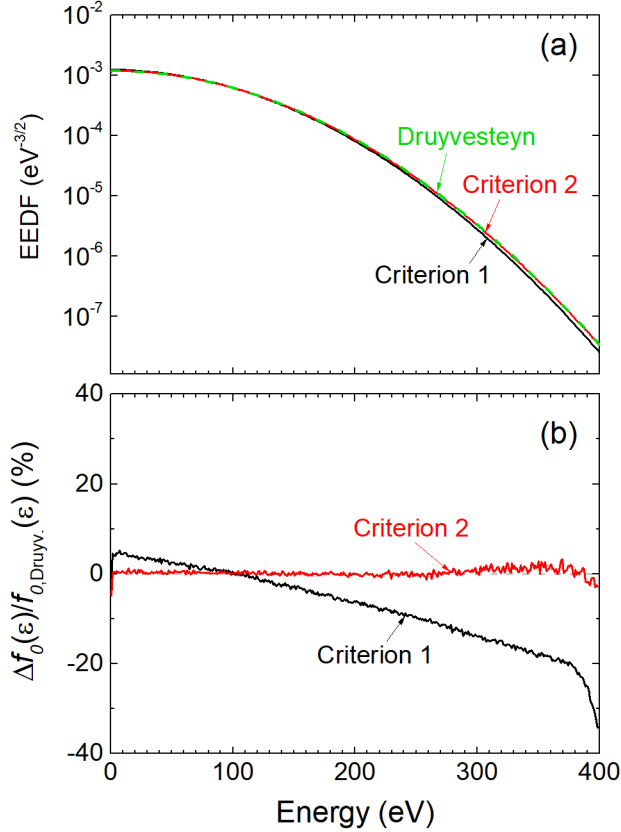


**Fig. 4.** (a) EEDFs calculated with MCF for a reduced electric field of 50 Td, elastic momentum transfer cross section  $\sigma = 2 \times 10^{-20} \text{ m}^2$  and  $\Delta\epsilon = 1 \text{ eV}$ . Criteria 1 (black solid line) and 2 (red solid line) are used for time step calculations. The analytical Druyvesteyn distribution (green dashed line) is also shown. (b) Percent error for MCF calculations with Criterion 1 and 2, with respect to the analytical Druyvesteyn distribution.

The algorithm for the adaptive estimation of  $\Delta t$  is a good compromise between computational efficiency and accuracy even in arbitrary complex chemistries, as it is shown in the next sections. More generally, this empirical criterion could be improved to make it applicable even to non-equally spaced meshes or with a more general consideration of energy and momentum relaxation frequencies [53]. The procedure is typically very fast (around milliseconds of CPU time) and performed just once, before the MC module is executed.

## 4.2 Code benchmarking

### *Legendre polynomial coefficients*

MCF calculations of Legendre polynomial coefficients were compared with results from the two-term solver BOLSIG+ [10] and the multi-term MultiBolt [31], with ten terms in the expansion. Simulations were performed in argon. Electron impact cross sections from the Biagi database (from MagBoltz code version 8.9 and higher) of LXCat [61] were used. Collisions include: elastic momentum transfer, ionization and 44 excitations by electron impact. The external reduced electric field along  $\hat{z}$ -direction ranges from 50 to 1500 Td. Isotropic inelastic scattering is considered. Elastic scattering is also treated isotropically with the use of the elastic momentum transfer cross section. After an ionization event, equal energy sharing between primary and secondary electrons is enforced. However, it should be taken into account that, for high electric fields, anisotropic scattering of elastic and inelastic scattering, as well as different energy sharing models for ionization should be considered. An example is proposed in [45] and [63] for treatment of anisotropic elastic scattering or in [64] where doubly differential cross sections are presented for the description of energy sharing in ionization events. Those techniques are implemented in the MCF code, but not in the current versions of the other two solvers used for benchmarking. For this reason, those treatments were not considered in MCF calculations presented here. After the calculation of transition probabilities with a short MC simulation, steady-state distribution functions are calculated with the eigenvalue method previously mentioned. MCF numerical parameters are reported in Table 1, where an initial uniform distribution of  $10^4$  electrons per cell is assumed. The MC time step  $\Delta t$  is calculated internally with the criteria illustrated in Section 4.1. Moreover, the CPU time of MCF simulations, reported in the last column, will be discussed later in this section.

**Table 1.** Numerical parameters and CPU time of MCF simulations for different reduced electric fields.

<b>E/N (Td)</b>	<b><math>\epsilon_{max}</math> (eV)</b>	<b><math>n_{cos\theta}</math></b>	<b><math>\Delta\epsilon</math> (eV)</b>	<b><math>n_c</math></b>	<b>CPU time (s)</b>
50	30.0	50	1.0	$10^4$	96.5
100	50.0	50	1.0	$10^4$	133.2
200	100.0	50	1.0	$10^4$	361.2
500	200.0	50	1.0	$10^4$	533.4

1500	500.0	50	1.0	$10^4$	636.9
------	-------	----	-----	--------	-------

In BOLSIG+ the default numerical parameters (precision:  $10^{-10}$ , convergence:  $10^{-5}$  and number of iterations: 2000) are used with equal energy sharing and temporal growth rate in the electron production and 100 energy intervals. Self-collisions of electrons (i.e. electron-electron collisions) are neglected in the present treatment, in order to analyze the linear Boltzmann problem. MultiBolt was run with a ten-term expansion in Legendre polynomials in hydrodynamic regime (see [31]). Numerical parameters are: Energy points: 1000, number of maximum iterations: 1000, convergence error in mean energy:  $5 \times 10^{-6}$ . In all simulations, the thermal motion of the background gas is neglected (i.e. zero temperature background). This is a reasonable assumption, due to the large difference between electron and heavy particle mass. However, the addition of this effect may have an impact at values of the reduced electric fields so low that the mean energy compares with thermal energy of the neutral gas, mainly due to the electron-neutral energy transfer involved in elastic collisions.

The first three Legendre polynomial coefficients ( $f_0$ ,  $f_1$  and  $f_2$ ) were considered. Because of the symmetry of the system, only these coefficients are used in the calculation of flux transport parameters like reduced mobility and components of the diffusion tensor [40]. Results for lower values of E/N (between 1 and 50 Td) were in excellent agreement with solutions of two-term and multi-term solvers (not shown), since the two-term approximation does not break down in such conditions.

In Fig. 5, results for the zeroth order Legendre polynomial coefficient ( $f_0$ ) are shown. As previously mentioned, this is the isotropic component or EEDF. For reduced electric fields greater than 200 Td, deviations from two-term calculations by BOLSIG+ can be observed. In fact, in those conditions, the small anisotropy approximation breaks down and the motion of electrons is strongly driven by the externally applied electric field. The presence of a strong electric field, in fact, has a double effect: it increases the contribution of inelastic collisions and sets a preferential direction in the motion of the electrons. Therefore, the small anisotropy assumption implicit in the two-term description is no longer valid and calculations with a multi-term solver or MC or MCF are necessary.

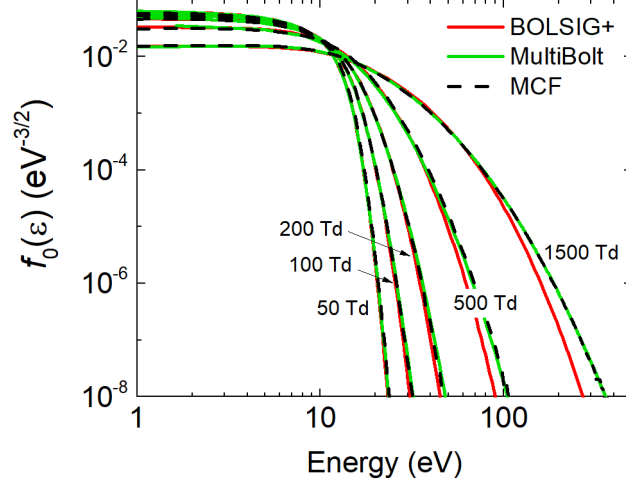


**Fig. 5.** Zeroth order Legendre polynomial coefficients calculated with MCF, BOLSIG+ (2-term solver) and MultiBolt (10-term solver) for argon at different constant reduced electric fields.

A comparison of the first order ( $f_1$ ) and second order ( $f_2$ ) Legendre polynomial coefficients is shown in Figs. 6 and 7. Analogously to the previous case, deviations from BOLSIG+ can be observed in  $f_1$ , due to the dependence of  $f_1$  on the isotropic component ( $f_0$ ) in the two-term formulation [65]. This implies that, in a two-term solver, approximations in the calculation of  $f_0$  propagate into the calculation of  $f_1$ . It is worth noting that, by increasing the reduced electric field to 1500 Td, the profile of  $f_1$  has a maximum around 15 eV and decreases with decreasing energy in the low energy region. This effect is due to the equal energy sharing assumed in ionization collisions. Different energy sharing models may result in different profiles more peaked at low energy. Moreover, an effect on the tail of the distribution is expected at high values for the reduced electric field when choosing a different energy partition model in ionization collisions [66]. MCF calculations of  $f_2$  can only be compared with results of MultiBolt, since this coefficient is not considered in the two-term description. The agreement of MCF with MultiBolt results is very good for  $f_0$ , but not for  $f_1$  and  $f_2$  at low energies, because of the different energy resolution assumed in the models. This problem can be overcome by decreasing the energy bin size used in MultiBolt at the cost of computational time. In this way, excellent agreement between MCF and MultiBolt results even in low energy region can be obtained (not shown).

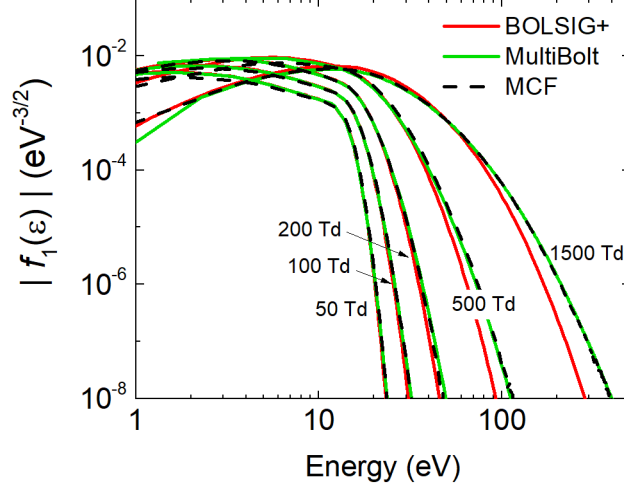


**Fig. 6.** First order Legendre polynomial coefficients calculated with MCF, BOLSIG+ (2-term solver) and MultiBolt (10-term solver) for argon at different constant reduced electric fields.

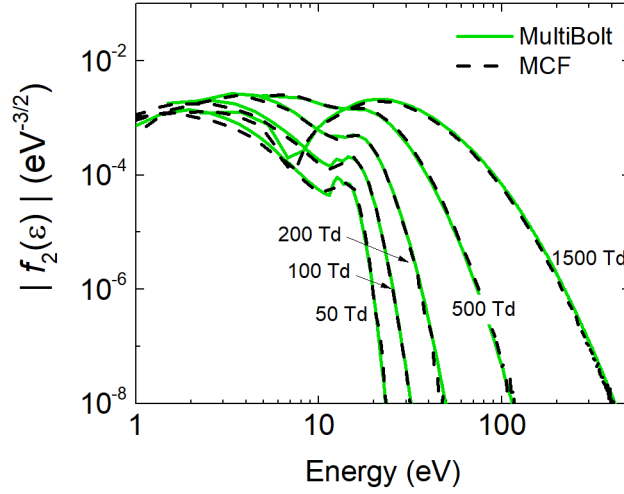


**Fig. 7.** Second order Legendre polynomial coefficients calculated with MCF and MultiBolt (10-term solver) for argon at different constant reduced electric fields.

The CPU time of MCF simulations (reported in Table 1) is determined mostly by the contribution of the MC and Markov chain modules. In the simulations, it was found that a number of  $10^4$  electrons per cell is a good compromise between accuracy and computational cost. Moreover, the eigenvalue solver of the LAPACK library used in the code becomes more computationally expensive by increasing the reduced electric field, due to the corresponding increase of the dimension of the Markov matrix. This is expected, since the solver makes no use of sparse matrices routines. Future improvements may involve a parallelization of the MC module and the use of a sparse matrix solver (e.g. ARPACK [67]). In this way, the CPU time could be decreased.

Furthermore, even though at this stage calculations with the other two solvers are much faster (within about 1 s with BOLSIG+ and about 30 s with MultiBolt), MCF provides an important reduction of CPU time when compared with MC simulations. This is shown later in this section for the case of time dependent calculations of the EEDF.

For completeness, a synoptic view of results for the first four Legendre polynomial coefficients is presented in Fig. 8 for a reduced electric field of 150 Td. MCF calculations are performed with  $10^5$  electrons per cell, energy bin size 0.5 eV, 100 bins in energy and 50 bins in  $\cos \theta$ . As mentioned before, deviations of results of BOLSIG+ in the isotropic and first anisotropic component of the distribution function show that higher order Legendre polynomial coefficients have an impact in regimes of strong anisotropy driven by the presence of the electric field. Furthermore, results for  $f_2$  and  $f_3$  show a good agreement between MCF and MultiBolt that is based on an expansion beyond the first harmonics. However, as opposed to a multi-term code, the MCF approach can be easily improved from the numerical point of view by exploiting straightforward parallel programming techniques and moreover, from the physical description point of view, it can be used to carry out studies of anisotropic effects on the distribution not feasible with deterministic solutions of the Boltzmann equation. In addition, the real power of MCF can be exploited when studying molecular gases, where an accurate description of electron kinetics beyond a two-term expansion is expected to be important for the calculation of chemical rate coefficients and transport parameters [28] or in cases where solutions are not well represented by an expansion in Legendre polynomials [68].

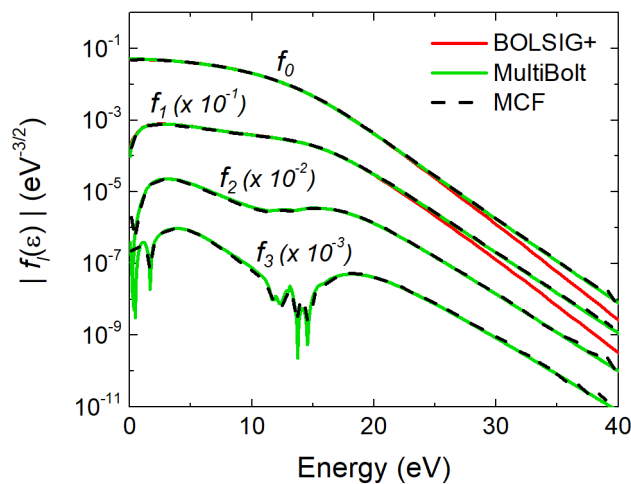


**Fig. 8.** First four Legendre polynomial expansion coefficients calculated in argon at 150 Td. MCF calculations are compared with BOLSIG+ (2-term solver) and MultiBolt (10-term solver) results. Note that

$f_2$  and  $f_3$  can only be obtained from MCF or a multi-term expansion. Results for  $f_1$ ,  $f_2$  and  $f_3$  are shifted downwards for readability.

### *Effect of superelastic collisions*

Superelastic collisions, that is collisions between electrons and a molecule/atom in an excited state leading to de-excitation with electrons gaining the energy lost in the transitions between excitation states, can affect electrons description depending on the applied reduced electric field and the number density of excited species. Since, at the moment, MCF is not coupled with a system of particle balance equations for the calculation of the population of excited states, the fraction of the number density of atoms in excited state and ground state  $N_m/N_0$  is used as a parameter and assumed as time independent. For simplicity, only superelastic collisions with the  $^3P_2$  metastable state (with an excitation energy of 11.55 eV) leading to a de-excitation to the ground state are considered. The cross section for this process is derived from the principle of micro-reversibility with the Klein-Rosseland formula [47], using the corresponding electronic excitation cross section. Cross sections for other electron impact scattering processes are the same as in the previous case. EEDFs calculated with MCF and BOLSIG+ are compared in Fig. 9 at 10 Td, for different number densities of atoms in the metastable excited state. In these conditions, BOLSIG+ results are assumed to be accurate for the description of chemistry in an atomic system. Moreover, a benchmarking with MultiBolt is not possible for this case, since the latter does not include a treatment of superelastic collisions. In MCF,  $10^5$  electrons were initially placed in each cell. Only a discretization in energy was considered with 100 energy bins with size 0.3 eV. BOLSIG+ simulations were run with default numerical parameters (precision:  $10^{-10}$ , convergence:  $10^{-5}$ , number of iterations: 2000 and 100 energy cells); Superelastic collision is enabled in the input file and number densities of atoms in the  $^3P_2$  and ground state are specified as input parameters. Excellent agreement between results from the two codes is obtained when superelastic collisions are neglected (i.e.  $N_m/N_0 = 0$  in the figure) and included. The increase of the number density of atoms in the  $^3P_2$  state affects the shape of the EEDF by enhancing the tail of the distribution. In this case, it was found that at least  $10^5$  electrons per cell are necessary in MCF simulations in order to properly describe the shape of the EEDF within 8 orders of magnitude. This is due to the large difference between the number of elastic and superelastic collisions electrons undergo, that can



reach several orders of magnitude in the energy range considered. Future improvements may include variance reduction techniques for the treatment of superelastic collisions, that could allow one to reduce the total number of simulated electrons.

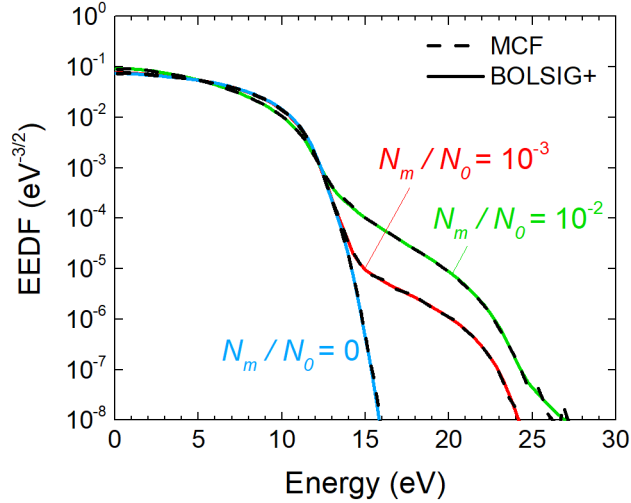


**Fig. 9.** EEDFs calculated in argon at 10 Td for different ratios of number densities of atoms in the  $^3P_2$  and in the ground state. MCF results (dashed line) are benchmarked against BOLSIG+ calculations (solid line).

### *Electron velocity distribution function*

In addition to Legendre polynomials expansion coefficients, MCF allows one to calculate full electron velocity distribution functions in (2). Given the symmetry of the system under examination, a two-dimensional velocity space with axial and radial velocity components with respect to the direction of the electric field was considered. An example of EVDF at 500 Td is shown in Fig. 10. Results have been calculated for  $10^4$  electrons distributed within an energy grid of 500 bins with size 1.0 eV and 50 angular bins. Results were smoothed out with the Dgrid function of gnuplot [69] in a grid of 50 rows and 50 columns corresponding to the radial and axial component respectively. In the corresponding contour plot in Fig. 11, it can be observed that the distribution is slightly asymmetric with a peak shifted in the direction opposite to the electric field. This effect is enhanced when increasing the reduced electric field (not shown), that provides a net drift of electrons. Drift and diffusion in velocity space can be inferred from this description, together with isotropic and anisotropic components of the Legendre expansion.

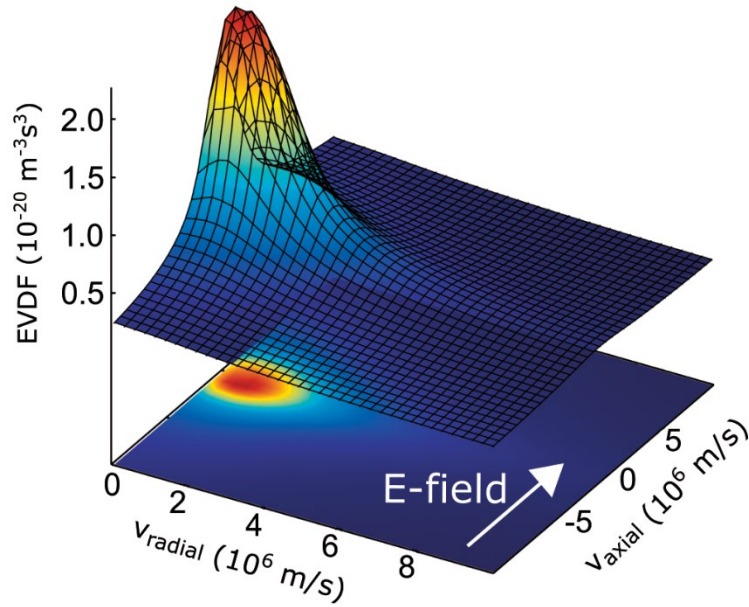


**Fig. 10.** Electron velocity distribution function as a function of axial and radial velocity components. Argon is used as background gas at a constant reduced electric field of 500 Td.

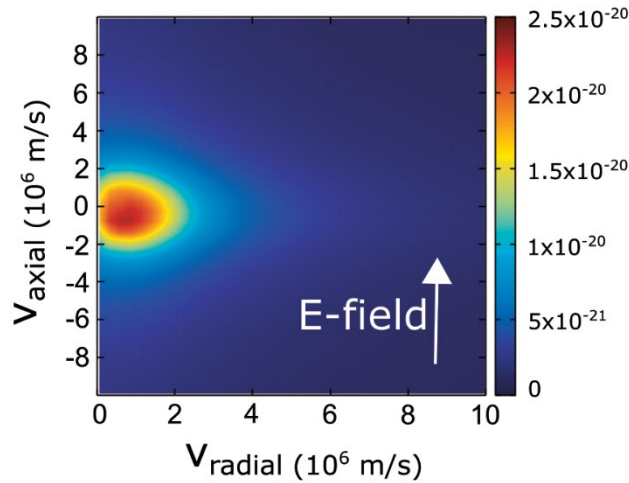


**Fig. 11.** Electron velocity distribution function calculated with MCF in argon at 500 Td, as a function of axial and radial velocity components (same conditions as Fig. 10).

### *Time evolution*

Results shown so far were related to steady-state solutions, however MCF is intrinsically time-dependent. As opposed to conventional MC simulations, where the time evolution is simulated

with a succession of several collisions for several physical times until steady-state is reached, in MCF simulations the EEDF can be evaluated with a time step  $\Delta t$  by the use of a Markov chain. In this way, transition probabilities are stored in the Markov matrix and iteratively applied to the initial distribution of electrons. A comparison between a MC and MCF results is shown in Fig. 12, for argon and a constant reduced electric field of 5 Td. In particular, it is shown how an initial distribution of electrons, placed in the first energy bin at  $t = 0$  s, evolves in time until it reaches steady-state. In conventional MC simulations,  $5 \times 10^6$  electrons were considered and, in this case, the accuracy of the EEDF is strongly affected by stochastic fluctuations below  $10^{-4}$  eV<sup>-3/2</sup>. This problem is overcome by MCF simulations with an initial distribution of  $10^4$  electrons per bin placed in 150 energy bins of size 0.1 eV for the calculation of transition probabilities. A time step  $\Delta t = 0.037$   $\mu$ s is used in the simulation, evaluated using criteria discussed in Section 2. Once transition probabilities are calculated and stored, the EEDF time evolution can be calculated deterministically with a time step  $\Delta t$ . In particular, the electron distribution is affected mainly by the contribution of the electric field and elastic collisions at 0.07  $\mu$ s, that is around  $2\Delta t$ . The EEDF is further populated at high energies as time elapses, until reaching steady-state, at around 18  $\mu$ s. This corresponds to approximately 500 times  $\Delta t$ . Since  $\Delta t$  is at least 2 orders of magnitude lower than the steady-state time, MCF is particularly effective in this case in reducing the number of simulated collisions with respect to a conventional MC. This reduction of simulated collisions is reflected in a direct decrease of CPU time, as reported in Fig. 13. While higher CPU times are associated with longer evolution times in MC simulations, due to the increasing number of collisions that has to be processed, CPU time in MCF simulations is around 30 s for all simulated physical times. This is due to the fact that transition probabilities are calculated just once and MC simulations are performed for the very short time  $\Delta t$ .

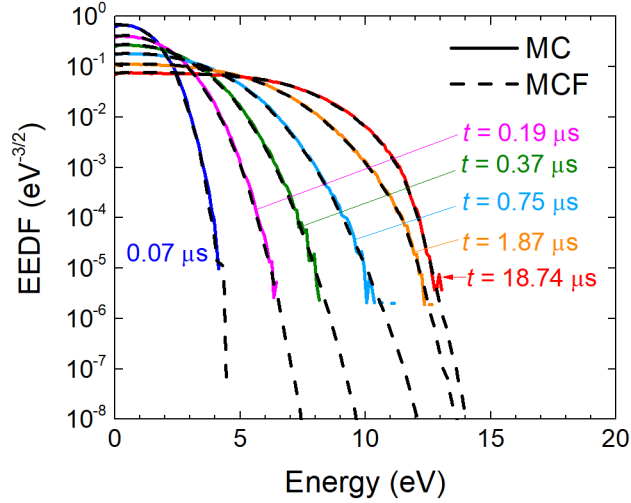


**Fig. 12.** EEDF evolution in argon at 5 Td from an initial distribution of electrons in the first energy bin. A time step of  $0.037 \mu\text{s}$  is used in MCF simulations for the calculation of transition probabilities.

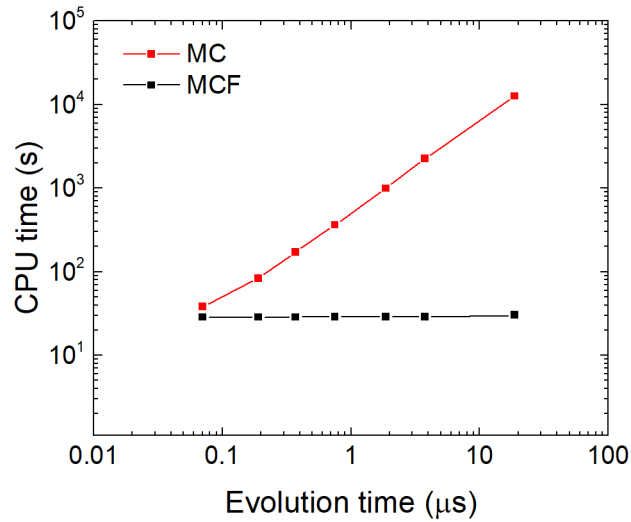


**Fig. 13.** MC and MCF CPU times for EEDFs calculation in argon for different evolution times and a constant reduced electric field of 5 Td (same conditions as Fig. 12).

## 5. Conclusions

In this work, the MCF method was reconsidered by means of an implementation carried out by the present authors. This reconsideration is in the perspective of a possible future integration of the method in more sophisticated chemical models describing plasma kinetics. In fact, nowadays those models require greater accuracy in the calculation of electron transport properties and chemical

rate coefficients, that are essential for a complete characterization of the discharge. In some cases, for example for applications to molecular gases or for high anisotropies in phase space, this requirement is not met by the widely used two-term approximation. At the same time, conventional MC approaches have a notoriously high computational cost. MCF is based on a straightforward idea, easy to implement, that keeps the essence of an MC simulation, but reduces drastically the number of simulated collisions. The price to pay is the assumption of a Markov property for the calculation of transition probabilities, that are strongly dependent on the choice of the MC time step. For this reason, it was shown that the method is more suitable for applications to complex chemistries with an improvement of the criterion for the calculation of the MC time step present in the original paper by Schaefer and Hui [44]. Results of the current implementation were also benchmarked against results from codes employing the two-term and multi-term approach. In particular, MCF provides more details than a two- and multi-term approach with the calculation of full electron velocity distribution functions; it is generally faster than a conventional MC and MCF results are in excellent agreement with results from a multi-term solver. Calculations were carried out in regimes of low and high reduced electric fields. In the latter case, ionization becomes important and would require, in principle, a more refined treatment than the one used here. In addition, representations of the Markov matrix were shown in order to give insight into the MCF method. In perspective, the current implementation of MCF is suitable for integration with complex chemistry modules that describe the time evolution of the kinetics of excited species. This is the focus of future works. Furthermore, the MCF method can be embedded in fluid and hybrid models for the calculation of electron rate coefficients and transport parameters. In this respect, it is worth to note that current approaches for fluid models solve the Boltzmann equation with the local field approximation. Non-local effects may be important in the case of a discharge confined in space where electrons diffuse from regions with different electric field. With future developments and extension of the method, MCF can become a powerful alternative to widely used MC codes to describe non-local effects in electron kinetics.

## **Acknowledgements**

The authors are grateful to Dr. E. Westerhof, Dr. P. Viegas from DIFFER and Dr. J. van Dijk from Eindhoven University of Technology for useful discussions. This work is part of the Shell-

NWO/FOM initiative 'Computational sciences for energy research' of Shell and Chemical Sciences, Earth and Life Sciences, Physical Sciences, FOM and STW.

## References

- [1] Massines F., Sarra-Bournet, C., Fanelli, F., Naudé, N. and Gherardi, N. Atmospheric pressure low temperature direct plasma technology: status and challenges for thin film deposition. *Plasma Processes Polym.* **9** (2012) 1041-73
- [2] Makabe T. and Petrović Z. Lj. *Plasma electronics: applications in microelectronic device fabrication*. CRC Press. 2014
- [3] Laroussi M. From killing bacteria to destroying cancer cells: 20 years of plasma medicine. *Plasma Processes Polym.* **11** (2014) 1138-41
- [4] Bongers W., *et al.* Plasma-driven dissociation of CO<sub>2</sub> for fuel synthesis. *Plasma Processes Polym.* **14** (2017) 1600126
- [5] Adamovich I., *et al.* The 2017 Plasma Roadmap: Low temperature plasma science and technology. *J. Phys. D: Appl. Phys.* **50** (2017) 323001
- [6] Bruggeman P. J., Iza F. and Brandenburg R. Foundations of atmospheric pressure non-equilibrium plasmas. *Plasma Sources Sci. Technol.* **26** (2017) 123002
- [7] Alves L. L., Bogaerts A., Guerra V. and Turner M. M. Foundations of modelling of non-equilibrium low-temperature plasmas. *Plasma Sources Sci. Technol.* **27** (2018) 023002
- [8] Robson R., White R. and Hildebrandt M. *Fundamentals of Charged Particle Transport in Gases and Condensed Matter*. CRC Press. 2017
- [9] Makabe T. Velocity distribution of electrons in time-varying low-temperature plasmas: progress in theoretical procedures over the past 70 years. *Plasma Sources Sci. Technol.* **27** (2018) 033001
- [10] Hagelaar G. J. M. and Pitchford L. C. Solving the Boltzmann equation to obtain electron transport coefficients and rate coefficients for fluid models. *Plasma Sources Sci. Technol.* **14** (2005) 722-33
- [11] <http://www.bolsig.laplace.univ-tlse.fr/> (last access 04/04/2019)
- [12] <http://plasimo.phys.tue.nl/> (last access 04/04/2019)
- [13] Dijk J. van, Peerenboom K. S. C., Jimenez-Diaz M., Mihailova D. B. and Mullen J. J. A. M. van der. The plasma modelling toolkit Plasimo. *J. Phys. D: Appl. Phys.* **42** (2009) 194012
- [14] S. Pancheshnyi, B. Eismann, G.J.M. Hagelaar, L.C. Pitchford, Computer code ZDPlasKin, <http://www.zdplaskin.laplace.univ-tlse.fr> (University of Toulouse, LAPLACE, CNRS-UPS-INP, Toulouse, France, 2008) (last access 04/04/2019)
- [15] Alves L. L. Fluid modelling of the positive column of direct-current glow discharges. *Plasma Sources Sci. Technol.* **16** (2007) 557-69

- [16] Ferreira C. M. and Loureiro J. Electron kinetics in atomic and molecular plasmas. *Plasma Sources Sci. Technol.* **9** (2000) 528-40
- [17] Loureiro J. Time-dependent electron kinetics in  $N_2$  and  $H_2$  for a wide range of the field frequency including electron-vibration superelastic collisions. *Phys. Rev. E* **47** (1993) 1262-75
- [18] Guerra V. and Loureiro J. Self-consistent electron and heavy-particle kinetics in a low-pressure-glow discharge. *Plasma Sources Sci. Technol.* **6** (1997) 373-85
- [19] Capitelli M., Colonna G., D'Ammando G. and Pietanza L. D. Self-consistent time dependent vibrational and free electron kinetics for  $CO_2$  dissociation and ionization in cold plasmas. *Plasma Sources Sci. Technol.* **26** (2017) 055009
- [20] Dyatko, N. A., Kochetov I. V. and Napartovich A. P. Electron energy distribution function in decaying nitrogen plasmas. *J. Phys. D: Appl. Phys.* **26** (1993) 418-23
- [21] Tejero-del-Caz A., Guerra V., Gonçalves D., da Silva M. L., Marques L., Pinhao N., Pintassilgo C. D. and Alves L. L. The LisOn KInetics Boltzmann solver. *Plasma Sources Sci. Technol.* **28** (2019) 043001
- [22] <https://github.com/IST-Lisbon/LoKI> (last access on 14/04/2019)
- [23] <https://fr.lxcat.net/download/EEDF/> (last access on 14/04/2019)
- [24] <https://github.com/aluque/bolos> (last access on 14/04/2019)
- [25] White R. D., Robson R. E., Dujko S., Nicoletopoulos P. and Li B., Recent advances in the application of Boltzmann equation and fluid equation methods to charged particle transport in non-equilibrium plasmas. *J. Phys. D: Appl. Phys.* **42** (2009) 194001
- [26] Ness K. F. and Robson R. E. Velocity distribution function and transport coefficients of electron swarms in gases. II. Moment equations and applications. *Phys. Rev. A* **34** (1986) 2185-209
- [27] Robson R. E. and Ness K. F. Velocity distribution function and transport coefficients of electron swarms in gases: spherical-harmonics decomposition of Boltzmann's equation. *Phys. Rev. A* **33** (1986) 2068-77
- [28] Pitchford L. C., O'Neil S. V. and Rumble Jr. J. R. Extended Boltzmann analysis of electron swarm experiments. *Phys. Rev. A* **23** (1981) 294-304
- [29] Dujko S., White R. D., Petrović Z. L. and Robson R. E. A multi-term solution of the non-conservative Boltzmann equation for the analysis of temporal and spatial non-local effects in charged-particle swarms in electric and magnetic fields. *Plasma Sources Sci. Technol.* **20** (2011) 024013
- [30] Leyh H., Loffhagen D. and Winkler R. A new multi-term solution technique for the electron Boltzmann equation of weakly ionized steady-state plasmas. *Comput. Phys. Commun.* **113** (1998) 33-48



- [31] Stephens J. A multi-term Boltzmann equation benchmark of electron-argon cross-sections for use in low temperature plasma models. *J. Phys. D: Appl. Phys.* **51** (2018) 125203
- [32] Longo S. Monte Carlo models of electron and ion transport in non-equilibrium plasmas. *Plasma Sources Sci. Technol.* **9** (2000) 468-76
- [33] Longo S. Direct derivation of Skullerud's Monte Carlo method for charged particle transport from the linear Boltzmann equation. *Phys. A* **313** (2002) 389-96
- [34] Longo S. Monte Carlo simulation of charged species kinetics in weakly ionized gases. *Plasma Sources Sci. Technol.* **15** (2006) S181-8
- [35] Yousfi, M., Hennad A. and Alkaa A. Monte Carlo simulation of electron swarms at low reduced electric fields. *Phys. Rev. E* **49** (1994) 3264-73
- [36] Kushner M. J. Monte-Carlo simulation of electron properties in rf parallel plate capacitively coupled discharges. *J. Appl. Phys.* **54** (1983) 4958-65
- [37] Boeuf J. P. and Marode E. A Monte Carlo analysis of an electron swarm in a non-uniform field: the cathode region of a glow discharge in helium. *J. Phys. D: Appl. Phys.* **15** (1982) 2169-87
- [38] Rabie M. and Franck C. M. METHES: A Monte Carlo collision code for the simulation of electron transport in low temperature plasmas. *Comput. Phys. Commun.* **203** (2016) 268-77
- [39] [www.lxcat.net/download/METHES](http://www.lxcat.net/download/METHES) (last access 04/04/2019)
- [40] Vass M., Korolov I., Loffhagen D., Pinhao N. and Donkó Z. Electron transport parameters in CO<sub>2</sub>: scanning drift tube measurements and kinetic computations. *Plasma Sources Sci. Technol.* **26** (2017) 065007
- [41] Penetrante B. M., Bardsley J. N. and Pitchford L. C. Monte Carlo and Boltzmann calculations of the density gradient expanded energy distribution functions of electron swarms in gases. *J. Phys. D: Appl. Phys.* **18** (1985) 1087-100
- [42] Petrović Z. Lj, Dujko S., Marić D., Malović G., Nikitović Ž., Šašić O., Jovanović J., Stojanović V. and Radmilović-Rađenović M. Measurement and interpretation of swarm parameters and their application in plasma modelling. *J. Phys. D: Appl. Phys.* **42** (2009) 194002
- [43] Dupree S. A. and Fraley S. K. *A Monte Carlo Primer: A Practical Approach to Radiation Transport*. Springer Science & Business Media. 2012
- [44] Schaefer G. and Hui P. The Monte Carlo flux method. *J. Comput. Phys.* **89** (1990) 1-30
- [45] Longo S. and Capitelli M. A simple approach to treat anisotropic elastic collisions in Monte Carlo calculations of the electron energy distribution function in cold plasmas. *Plasma Chem. and Plasma Process.* **14** (1994) 1-13

- [46] Wu C.-H. J., Li C. C., Tsai J. H. and Young F. F. Solving the Boltzmann equation in a 2-D configuration and 2-D-velocity space for capacitively coupled RF discharges. *IEEE Trans. Plasma Sci.* **23** (1995) 650-60
- [47] Capitelli M., Celiberto R., Colonna G., Esposito F., Gorse C., Hassouni K., Laricchiuta A. and Longo S. *Fundamental Aspects of Plasmas Chemical Physics: Kinetics* 85. Springer Science & Business Media. 2015
- [48] Cercignani C. *Mathematical methods in kinetic theory*. New York: Plenum Press. 1969
- [49] Landau L. D., Lifshitz E. M. and Pitaevskij L. P. *Course of theoretical physics. vol. 10: Physical kinetics*. Oxford: Butterworth-Heinemann. 1981
- [50] White R. D., Robson R. E., Schmidt B. and Morrison M. A. Is the classical two-term approximation of electron kinetic theory satisfactory for swarms and plasmas?. *J. Phys. D: Appl. Phys.* **36** (2003) 3125-31
- [51] Braglia G. L. and Romanò L. Monte Carlo and Boltzmann two-term calculations of electron transport in CO<sub>2</sub>. *Lettere al Nuovo Cimento (1971-1985)* **40** (1984) 513-8
- [52] Skullerud H. R. The stochastic computer simulation of ion motion in a gas subjected to a constant electric field. *J. Phys. D: Appl. Phys.* **1** (1968) 1567-8
- [53] Capitelli M., Ferreira C. M., Gordiets B. F. and Osipov A. I., *Plasma kinetics in atmospheric gases* (Vol. 31). Springer Science & Business Media. 2013
- [54] Van Kampen N. G. *Stochastic processes in physics and chemistry*. Vol. 1. Elsevier. 1992
- [55] Eastwood J. W., Hockney R. W. *Computer Simulation using particles*. New York: Mc GrawHill. (1981)
- [56] Nishimura T. Tables of 64-bit Mersenne twisters. *ACM Trans. Model. Comput. Simul. (TOMACS)* **10** (2000) 348-57
- [57] Matsumoto M. and Nishimura T. Mersenne twister: a 623-dimensionally equidistributed uniform pseudo-random number generator. *ACM Trans. Model. Comput. Simul. (TOMACS)* **8** (1998) 3-30
- [58] <http://www.math.sci.hiroshima-u.ac.jp/~m-mat/MT/emt.html> (last access 04/04/2019)
- [59] <http://www.netlib.org/lapack/> (last access 04/04/2019)
- [60] [https://people.sc.fsu.edu/~jburkardt/f\\_src/sparsekit/sparsekit.html](https://people.sc.fsu.edu/~jburkardt/f_src/sparsekit/sparsekit.html) (last access 04/04/2019)
- [61] Biagi database, [www.lxcat.net](http://www.lxcat.net), retrieved November 5, 2018
- [62] Dujko S., White R. D., Petrović Z. L. and Robson R. E. Benchmark calculations of non-conservative charged-particle swarms in dc electric and magnetic fields crossed at arbitrary angles. *Phys. Rev. E* **81** (2010) 046403

- [63] Okhrimovskyy A., Bogaerts A. and Gijbels R. Electron anisotropic scattering in gases: A formula for Monte Carlo simulations. *Phys. Rev. E* **65** (2002) 037402
- [64] Opal C. B., Peterson W. K. and Beaty E. C. Measurements of secondary-electron spectra produced by electron impact ionization of a number of simple gases. *J. Chem. Phys.* **55** (1971) 4100-6
- [65] Braglia G. L., Wilhelm J. and Winkler R. Monte Carlo and Boltzmann calculations of the time-dependent velocity distribution of electrons in an electric field in a gas. *Il Nuovo Cimento D* **16** (1994) 411-5
- [66] Yoshida S., Phelps A. V. and Pitchford L. C. Effect of electrons produced by ionization on calculated electron-energy distributions. *Phys. Rev. A* **27** (1983) 2858-67
- [67] <https://www.caam.rice.edu/software/ARPACK/> (last access 15/04/2019)
- [68] Allis W. P. Semidivergence of the Legendre expansion of the Boltzmann equation. *Phys. Rev. A* **26** (1982) 1704-12
- [69] [http://gnuplot.sourceforge.net/docs\\_4.2/node177.html](http://gnuplot.sourceforge.net/docs_4.2/node177.html) (last access 14/04/2019)